A Study on the Enhancement of Available Transfer Capability Using the Flexible AC Transmission System (FACTS)

Jae-Hyeon Gim †, Yang-Il Kim* and Sung-Won Jeung*

Abstract - This paper evaluates FACTS control on the available transfer capability (ATC) enhancement. Technical merits of FACTS technology on boosting ATC are analyzed. More effective control means for line flow and bus voltage require the application of FACTS. In this paper, the power flow calculation method for the power systems with FACTS is based on the current injection model (CIM) and the Newton-Raphson method. An integrated scheme for ATC calculation, which considers the dynamic characteristic of the power system, is suggested. The study is applied to the IEEE 57-bus power system to demonstrate the effectiveness of FACTS control on ATC enhancement.

Keywords: ATC, FACTS, Power Flow, Stability

1. Introduction

Along with the reconstruction of the electrical power industries has been the implementation of new dispatch systems complying with the economical rule in the power market. The old energy management systems (EMSs) had been the function of the economical allocation of generation and network security, but following the reconstruction of power system operation, the industries started to focus more attention on the profitability aspect. In order to maximize commercial usage of the network within their limitations, the additional transfer capacity of the transmission network apart from the current transfer value is significant. The amount of this unused capacity at a given time is called ATC. Various approaches for calculating ATC are suggested [1, 2], however, some uncertainties remain during this process.

The increasing load and difficulties in transmission line construction on the power system has the transmission system nearly reaching its limit. Thus, effective control of power flow has become crucial. A method of supplementing the transmission system is the installation of FACTS to increase the power flow. FACTS can regulate both bus voltage and line flow giving it flexibility, effectiveness, and diversity in its application. These advantages led to the application expansion of FACTS.

For power system operation utilizing FACTS, a steady state analysis is required, which is a power flow calculation The power flow calculation in reference [5] uses the mismatches between the specified and calculated values to adjust the state variables converging to a solution. This method is simple and doesn't require modification, but the convergence speed is slow. The method using sensitivity [6] and distribution factors [7] improved the convergent characteristics. The automatic control method using controlled variables as independent variables were applied [8]. However, these methods need revision of the Jacobian matrix.

Since the power flow of the power system with FACTS does not always obtain the solution using the classical calculation method [8, 9], it is difficult to analyze the effects of FACTS on a power system. In order to control the management of FACTS, it is necessary to have the solution method for each control parameters and its models

For transient stability analysis, the dynamic models of UPFC consist of two equivalent voltage sources using converters to regulate the voltage magnitude and angle. The series injection voltage, V_{se}, controls the active and reactive power flow of the transmission line, and the shunt injection voltage, V_{sh}, controls the bus voltage, to which the UPFC is connected. Reference [11] suggests a closed loop feedback control of active and reactive power of the transmission line. Reference [12] proposed a method that separates two components to control both active and reactive power flow.

For static available transfer capability calculation, there are several methods: the continuous power flow methods [2, 14], the repeated power flow method, and the optimal power flow method [15], which considers security. Otherwise, the study for dynamic available transfer capability calculation with transient stability constraints is in its beginning stages.

This paper proposes a method to control several FACTS for power flow calculation using the current injection

The Transactions of the KIEE, Vol.53A, No.8, AUG. 2004, pp.446-453 : A paper recommended and approved by the Editorial Board of the KIEE Power Engineering Society for translation for the KIEE International Transaction on PE.

† Corresponding Author: Dept. of Electrical Control Engineering, Sunchon National University, Korea. (jhg@sunchon.ac.kr)

* Dept. of Electrical Control Engineering, Sunchon National University, Korea. (lime@sunchon.ac.kr, ww180@sunchon.ac.kr)

Received Jun 7, 2004 ; Accepted July 5, 2004

model (CIM) and the Newton-Raphson method. Using the static available transfer capability, the integrated calculation scheme of dynamic available transfer capability is suggested. It is then applied to the IEEE 57-bus system to analyze the effect of FACTS on the available transfer capability.

2. UPFC Model

2.1 Current Injection Model for UPFC

The UPFC is connected to the power system by the transformers and has the shunt converter and the series converter as shown in Fig. 1. The basic function of the shunt converter via the transformer is to supply or absorb the real power demanded by the series converter at the common dc link. The series converter is used to inject the required series voltage to control the transmission line flow. The transformer impedance is z_{se} for the series converter and z_{sh} for the shunt converter.

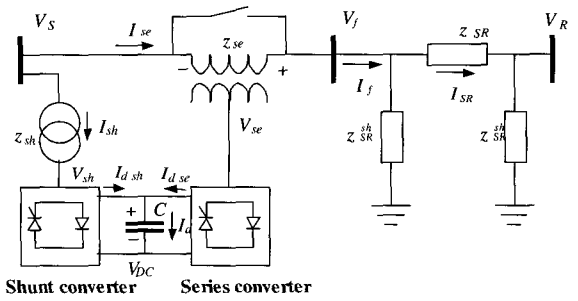

Fig. 1 Structure of UPFC

SSSC is the UPFC without the shunt device and STATCOM is the UPFC without the series device. TCPS regulates the phase angle of the series device and TCSC adjusts the impedance. This means that UPFC is a combination of STATCOM and SSSC.

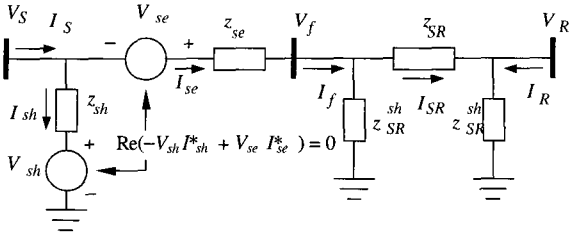

Fig. 2 Equivalent circuit of UPFC

Fig. 2 indicates the two equivalent circuits for UPFC, which have series and shunt. Since the UPFC does not absorb and generate real power, it is necessary to meet the active power balance neglecting device losses as shown in Eq (1).

$$Re(-V_{sh}I_{sh}^{*} + V_{se}I_{se}^{*}) = 0 \tag{1}$$

There is the vector diagram of UPFC as shown in Fig. 3. The series injected voltage V_{se} can be split into two components; one component of magnitude V_{sep} in phase with V_S and another component of magnitude V_{seq} in quadrature with V_S. The shunt current I_{sh} is also split into two components: a reactive current I_{shq} in quadrature with bus voltage V_S and a real current I_{shp} in phase with V_S.

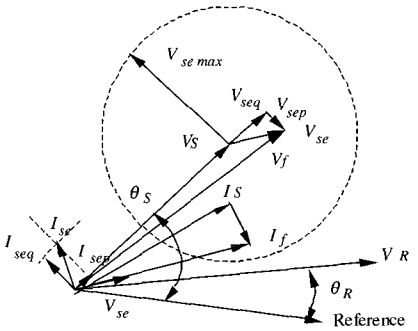

Fig. 3 Vector diagram of UPFC

The current I_{shp} is to maintain the capacitor voltage and power balance requirements between the two converters as in Eq. (2)

$$Re(V_S I_{shp}^{*} + V_{se}I_{se}^{*}) = 0 \tag{2}$$

From Eq. (2), the magnitude of the shunt real current is

$$I_{shp} = \frac{Re(V_{se}I_{se}^{*})}{|V_S|} \tag{3}$$

In Fig. 2, the current of bus f is

$$\begin{aligned} I_{se} &= I_f \\ &= (y_{SR} + y_{SR}^{sh})(V_S + V_{se} - Z_{se}I_{se}) - y_{SR}V_R \end{aligned} \tag{4}$$

where y_{SR} is $1/z_{SR}$ and y_{SR}^{sh} is $1/z_{SR}^{sh}$. Rearrange Eq. (4)

$$I_{se} = \frac{(y_{SR} + y_{SR}^{sh})(V_S + V_{se}) - y_{SR}V_R}{1 + (y_{SR} + y_{SR}^{sh})Z_{se}} \tag{5}$$

Therefore, the current I_S of bus S is

$$\begin{aligned} I_S &= I_{sh} + I_f \\ &= I_{sh} + (y_{SR} + y_{SR}^{sh})(V_S + V_{se} - Z_{se}I_{se}) - y_{SR}V_R \end{aligned} \tag{6}$$

Substituting Eq. (5) into Eq. (6), the injection current of the sending end is

$$I_S = I_{sh} + Y_{SS}(V_S + V_{se}) - Y_{SR}V_R \tag{7}$$

where

$$Y_{SS} = \frac{y_{SR} + y_{SR}^{sh}}{1+(y_{SR} + y_{SR}^{sh})z_{se}}$$

$$Y_{SR} = \frac{y_{SR}}{1+(y_{SR} + y_{SR}^{sh})z_{se}}$$

The injected current of the receiving end is

$$\begin{aligned} I_R &= y_{SR}(V_R - V_f) + y_{SR}^{sh}V_R \\ &= y_{SR}[V_R - (V_S + V_{se} - z_{se}I_{se})] + y_{SR}^{sh}V_R \end{aligned} \tag{8}$$

Substituting Eq. (5) into Eq. (8)

$$\begin{aligned} I_R = &-Y_{SR}V_S - Y_{SR}V_{se} \\ &+\left[y_{SR}^{sh} + \frac{y_{SR}(1+y_{SR}^{sh}z_{se})}{1+(y_{SR} + y_{SR}^{sh})z_{se}} \right] V_R \end{aligned} \tag{9}$$

Fig. 4 indicates the current injection model for UPFC using Eq. (7) and Eq. (9). This model can be applied to all other FACTS except the TCSC. For the TCSC, the injection model must be modified by z_{se}. This paper does not deal with the TCSC.

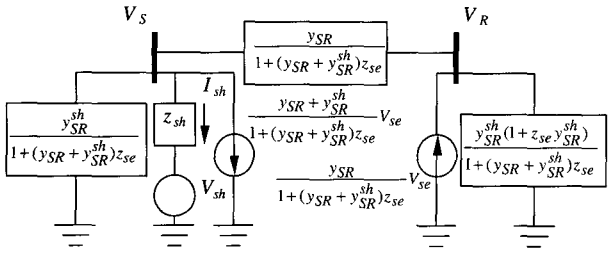

Fig. 4 The current injection model for UPFC

When the current injection model of UPFC is used, there are several advantages. The symmetrical admittance matrix is not changed. The other types of FACTS can represent the equivalent current source like generators and loads. The current source of UPFC regulates the power flow of the transmission line as an independent variable. The current injection model does not need to change the Jacobian matrix for power flow calculation. The current injection for FACTS is considered as the bus mismatch of power flow calculation. The current source of control variable for FACTS can be changed easily depending on each type.

The power flow between bus S and bus R is a function of their voltage and injection current when the injection current is used to control variables. The injection current is like generators and loads but regulates the power flow of the transmission line. The injection current for series converter, I_{se} and that of shunt converter, I_{sh} must be added for bus S. The series voltage, V_{se}, and the shunt voltage, V_{sh} for current injection are calculated by the Newton method with specified conditions.

2.2 Dynamic Model for UPFC

In Fig. 1, the dynamic characteristic of UPFC must represent the capacitor voltage variation on the DC side. The dynamic model for UPFC in Reference [17, 18] is used. The relations between the voltage and the current for UPFC is

$$I_d = C\frac{dV_{dc}}{dt} \tag{10}$$

$$I_d = I_{dsh} + I_{dse} \tag{11}$$

Active power on DC terminal of the converter

$$P_{sh} = V_d I_{dsh} / S_B \tag{12}$$

$$P_{se} = V_d I_{dse} / S_B \tag{13}$$

If the converters are ideal, active power on the AC terminal is equal to that on the DC terminal.

$$P_{sh} = Re(V_{sh}I_{sh}^*) \tag{14}$$

$$P_{se} = Re(V_{se}I_{se}^*) \tag{15}$$

The PWM control technique is applied to both of the voltage source converters so that the relation between the converter DC and AC side voltage is;

$$V_{sh} = m_{sh}V_{dc} / V_B \tag{16}$$

$$V_{se} = m_{se}V_{dc} / V_B \tag{17}$$

Where m_{sh} and m_{se} are PWM coefficients to maintain the voltage magnitude, V_{sh} and V_{se}. The phase angles, θ_{sh} and θ_{se}, are the phase differences between the voltage angle, θ_S, of bus S and firing angles, ϕ_{sh} and ϕ_{se}, respectively.

$$\theta_{sh} = \theta_S - \phi_{sh} \tag{18}$$

$$\theta_{se} = \theta_S - \phi_{se} \tag{19}$$

From Eq. (10), the dynamic model for UPFC is

$$CV_d \frac{dV_{dc}}{dt} = (P_{sh} - P_{se})S_B \tag{20}$$

This model can be applied to multi-machine power systems and various control schemes. The voltage magnitude and angle of the converters are controlled by m_{sh}, ϕ_{sh} and m_{se}, ϕ_{se}.

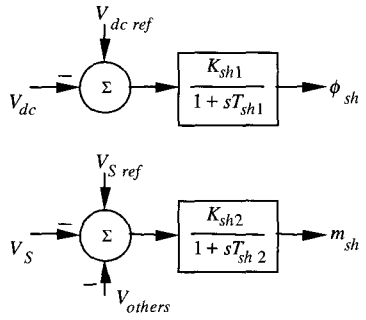

Fig. 5 Shunt Converter Controller

The shunt element control functions when the constant DC link capacitor voltage control is realized by controlling the firing angle ϕ_{sh} of the shunt converter, and the constant AC bus voltage control achieved by controlling m_{sh} of the PWM controller of the shunt converter. In order to improve system damping, a supplementary control is added with its output V_{others} used to modulate the terminal bus voltage

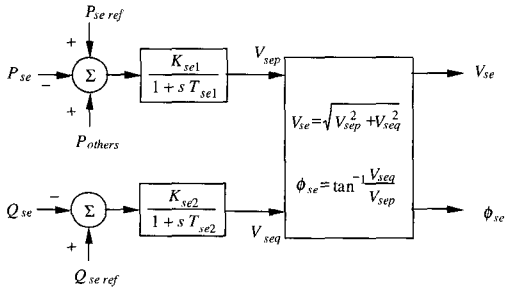

Fig. 6 Series Converter Controller

Obviously, these two components have strong impacts on active and reactive power flow, respectively. The inserting voltage magnitude and angle in Fig. 6 can be decomposed to V_{sep} and V_{seq}. V_{sep} and V_{seq} from the PI controllers. The former is perpendicular to V_S, and the latter is in phase with V_S as discussed in section 2.1. The input of the PI controller is the difference between the reference value and current value for active and reactive power. The output of series converter voltage, V_{se}, must be within the definite limit of V_{semax}.

3. ATC

The ATC is the viable increase in real power transfer from one point to another in a power system. This is useful information for system operators as an index of the power transfer margin.

The transmission networks to reliably transfer electric power may be limited by thermal limits of transmission lines and transformers, voltage limits of all buses, and stability limits of all generators. ATC is also limited by the three factors in this paper. Each have been considered accordingly: power flow calculation for thermal limits, voltage stability analysis for voltage limits, and transient stability analysis for stability limits as shown in Fig. 7. The possible λ value for TTC is derived using the power flow calculation. The λ is reduced until the voltage stability margin is sufficient from the voltage stability analysis. The λ is then evaluated for the stability limit using the transient stability analysis. There is the resulting a maximum λ, which satisfies all three limitations.

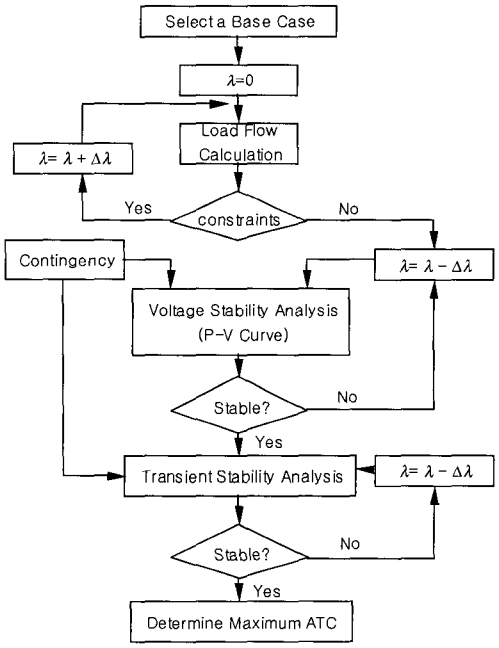

Fig. 7 Flow chart for total transfer capability

$$\text{ATC} = \text{TTC} - \text{TRM} - \text{CBM} - \text{ETC} \tag{21}$$

The TTC is the amount of electric power that can be transferred over the interconnected transmission network in a reliable manner while meeting all of a specific set of defined pre- and post- contingency system conditions.

Capacity Benefit Margin (CBM) is the amount of transmission transfer capability reserved by load serving entities to ensure access to generation from interconnected systems to meet generation reliability requirements. Existing Transmission Commitments (ETC) is the sum of all normal transmission flows included in the given cases.

At steady state, the ATC calculation method has several methods, but the following methods are mainly used.

1) Continuation power flow method (CPF)[11, 12]

2) Repeated power flow method (RPF)

3) Security constrained optimal power flow (SCOPF)

Static ATC calculation uses the RPF method in this paper. The procedure is as follows;

Objective function λ

Subject to

$$P_{Gi} - P_{Di} - \sum_{j=1}^{N} V_i V_j (G_{ij} \cos\delta_{ij} + B_{ij} \sin\delta_{ij}) = 0 \quad (22)$$

$$Q_{Gi} - Q_{Di} - \sum_{j=1}^{N} V_i V_j (G_{ij} \sin\delta_{ij} - B_{ij} \cos\delta_{ij}) = 0 \quad (23)$$

$$V_i \min \le V_i \le V_i \max \quad (24)$$

$$S_{ij} \le S_{ij} \max \quad (25)$$

where λ is the multiplier for generations and loads. (λ =0 at base case, $\lambda = \lambda_{max}$ at maximum transfer power)

P_{Gi}, Q_{Gi} : active and reactive power for generation at bus i

P_{Di}, Q_{Di} : active and reactive power for load at bus i

V_i, V_j : terminal voltage at buses i and j

G_{ij}, B_{ij} : admittance matrix elements

δ_{ij} : phase angle between buses i and j

V_{imax}, V_{imin} : maximum and minimum voltage at bus i

N : the number of buses

S_{ij} : apparent power at transmission line ij

From Eqs. (22) and (23), P_{Gi}, P_{Di} and Q_{Di} are given by the following equations.

$$P_{Gi} = P_{Gi}^0 (1 + \lambda K_{Gi}) \quad (26)$$

$$P_{Di} = P_{Di}^0 (1 + \lambda K_{Di}) \quad (27)$$

$$Q_{Di} = Q_{Di}^0 (1 + \lambda K_{Di}) \quad (28)$$

where P_{Gi} : active power generation of bus i at the base case

P_{Di}, Q_{Di} : active and reactive load of bus i at the base case

K_{Gi}, K_{Di} : weighting factor for generators and loads

In this case TTC is

$$TTC = \sum_{i \in Load\ Area} P_{Di}(\lambda_{max}) \quad (29)$$

$$ETC = \sum_{i \in Load\ Area} P_{Di}^0 \quad (30)$$

The maximum λ is calculated accordingly. In this paper, TRM and CBM are neglected for ATC calculation.

$$ATC = \sum_{i \in Load\ Area} P_{Di}(\lambda_{max}) - \sum_{i \in Load\ Area} P_{Di}^0 \quad (31)$$

The ATC between areas can be calculated by adjusting K_{Gi} and K_{Di} of each area or each bus.

The performance index π in reference [16] is used for contingency selection. This index includes the overloading index for transmission lines and the abnormal voltage index for buses.

4. Simulation Results

4.1 Test power system

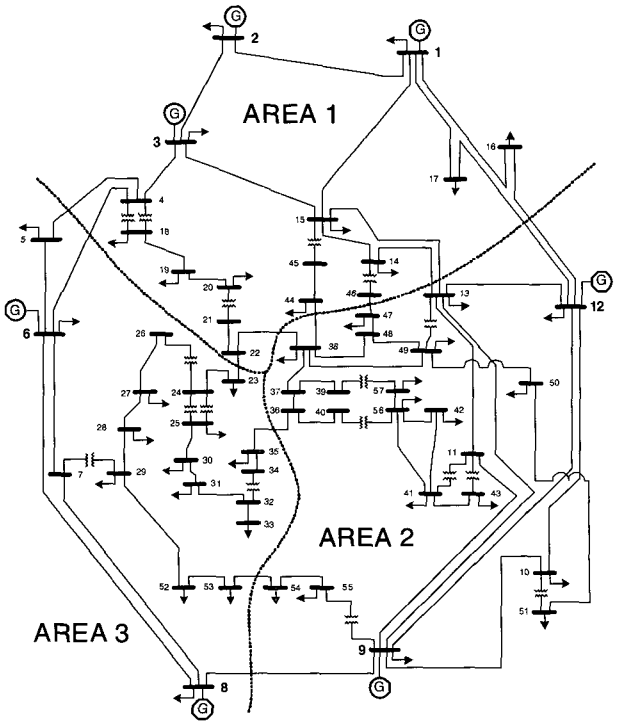

Fig. 8 IEEE 57 bus power system

The methods for enhancing ATC using FACTS have been tested on the IEEE 57 bus power system as shown in Fig. 8. The power system is divided into 3 areas. To

determine power transfer capability, the following constraints are assumed;

(1) The voltage of all buses must lie within the range of 0.9 to 1.1[p.u]
(2) Thermal capacity for transmission lines must be less than the specified MVA rating.
(3) For increasing the ATC, the weighting factors for generators and loads are identical.

At the base case, the voltage magnitude of all buses is in the range of 0.95 to 1.05 and there are no overloading branches. Table 1 represents the generation and load of each area at the base case. The transfer power is 182.4[MW] between area 1 and 2, 168.3[MW] between area 2 and 3, and 24.4[MW] between area 1 and 3 as shown in Table 2.

Table 1 Generation and load of each area

Area	Generation [MW/MVAR]	Load [MW/MVAR]	S.C [MVAR]
1	481.1/167.6	261.3/160.5	4.9
2	330.0/103.8	671.3/114.6	0.0
3	470.0/44.3	323.1/60.8	14.8
Total	1281.1/315.7	1255.7/335.9	19.7

Table 2 Transfer power between areas

Area	1	2	3
1	-	182.4/6.46	24.4/-0.5
2	-180.0/-8.9	-	-164.6/12.0
3	-24.3/-5.2	168.3/0.8	-

4.2 Results and Discussion

The study for power flow and voltage stability used the static voltage margin in the *P-V* curve. In this study, though the operating point is moved by disturbance, the voltage stability margin of the power system has to be secured sufficiently. When the power system is unstable, the FACTS device is used to improve the voltage stability. If the power system is still unstable, λ is reduced until the system becomes stable.

If the power system has adequate voltage stability margin, the study moves to transient stability. The models for the transient stability include the dynamic characteristic of the power system with the FACTS controller. The angle of the generator as well as the recovery of the bus voltage is considered for the stability analysis. The unstable phenomenon of transient stability analyzes the first swing and the dampening of the generator angle. The system runs on three phase faults for this study.

CASE 1: This case raises the transfer power by increasing the generation and load at the same rate. The result is that λ is increased until 0.407 and the lowest voltage bus is 34. This means that the total load of the system is increased up to 40.7[%]. Table 3 presents the transfer power of each area. Fig. 9 shows the relation of bus voltage and λ signifying incremental active power. When the bus voltage constraints are under 0.9[p.u], λ is 0.19. The bus voltage in Fig. 9 jumped, due either to transformer tap change and/or shunt capacitor adjustment.

Table 3 Transfer power between areas

Area	1	2	3
1	-	218.2/15.6	29.83/7.375
2	-214.7/-13.7	-	-193.65/14.4
3	-29.7/-12.7	199.1/6.8	-

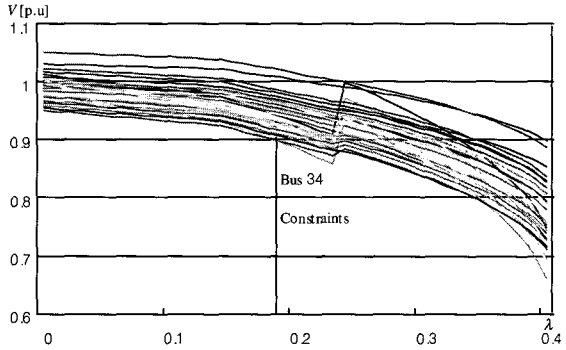

Fig. 9 Bus voltage versus λ curve

CASE 2: In this case, the disturbance of opening the line between bus 8 and bus 9 has occurred on the base case and

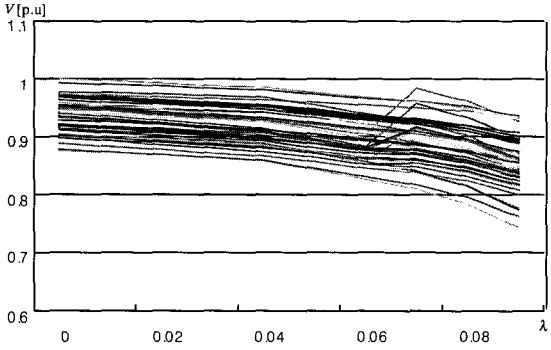

Fig. 10 Bus voltage versus λ curve with a disturbance (line open)

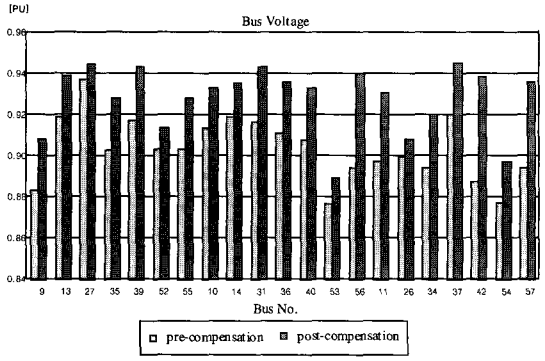

Fig. 11 Compensation STATCOM on bus 43 (line open)

heavy load. The abnormal status of the system is 14 overload transmission lines around the fault area and 34 low voltage buses. This resulted in increasing up to 0.91 as shown in Fig. 10.

Fig. 11 depicts the effect of voltage compensation when the shunt compensator is installed on bus 43.

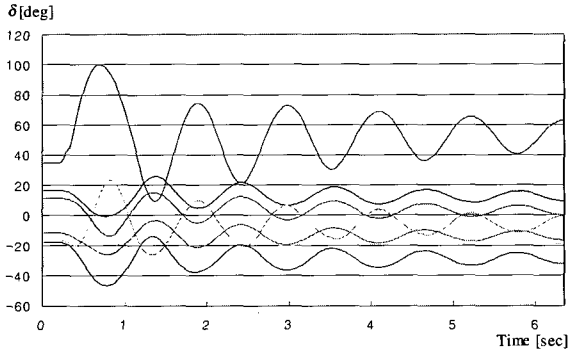

Fig. 12 Generator angle of base case (Line 8-9 fault)

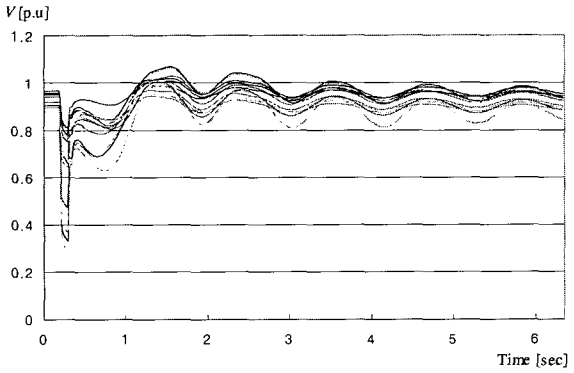

Fig. 13 Bus voltage magnitude (Line 8-9 Fault)

Fig. 12 illustrates the generator angle at the base case when a disturbance (three phase faults) occurred on the transmission line (bus8-bus9). The disturbance occurred at 0.2 sec, sustained for 0.08 sec (5Hz) and cleared. The results are that the oscillation of the generator angle dampened gradually. Fig. 13 shows that the bus voltage dropped during 1sec, then recovered and oscillated.

Figs. 14 and 15 demonstrate the generator angle and the bus voltage. The results illustrate that the generator angle is separated in two groups (generator #8 and the others) and the bus voltage is oscillated severely. This means that the power system is unstable. To make the power system stable, UPFC with the following data is installed on the transmission line between bus 29 and bus 52. The result is stable as seen in Fig. 16.

$$T_w = 0.3,\ K = 100,\ T_1 = 0.1,$$
$$T_2 = 0.2,\ T_3 = 0.1,\ T_4 = 0.2$$

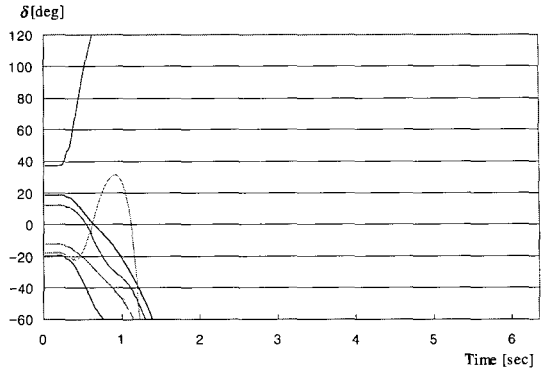

Fig. 14 Generator angle (λ=0.91)

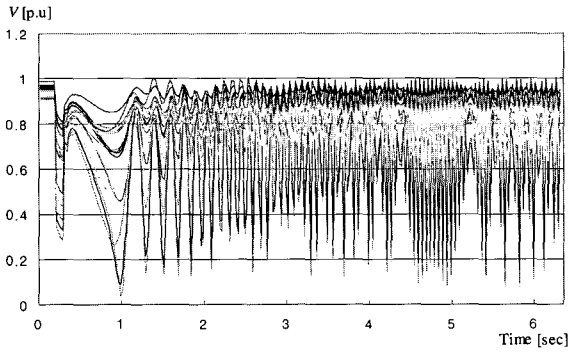

Fig. 15 Bus voltage (λ=0.91)

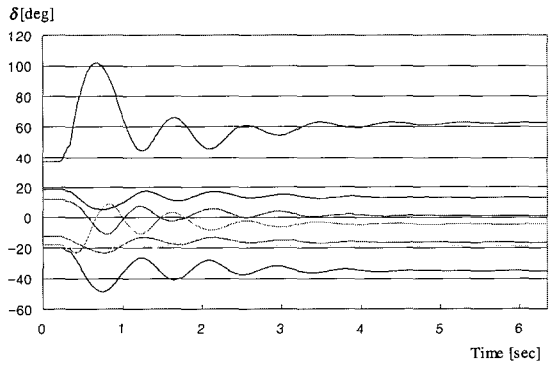

Fig. 16 Generator angle with FACTS (UPFC)

CASE 3: In this case, the generation in area 1 and the load in area 2 are increased. To maintain the balance of generation and load, K_{Gi} of the weighting factor of the generation in Eq. (26) is 1.0 and K_{Di} of the weighting factor of load in Eq. (27) is 0.805. λ is increased to 0.636, but when the bus voltage is above 0.9[p.u], λ is only increased to 0.275 as illustrated in Fig. 17. λ of this case is less than that of case 1. Table 4 indicates the transfer power between areas. The result shows that the transfer power is 317.1[MW] between area 1 and area 2 and 43.84[MW] between area 1 and area 3. The reason is so that the generation power in area 1 is transferred to the load in area 2 using the transmission network in area 3.

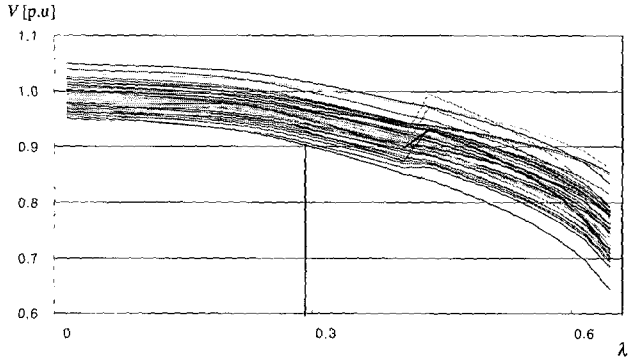

Fig. 17 Bus voltage versus λ curve

Table 4 Transfer power between areas

Area	1	2	3
1	-	317.10/14.39	43.84/-0.63
2	-310.96/-1.93	-	-183.10/-0.19
3	-43.56/-4.24	187.72/17.93	-

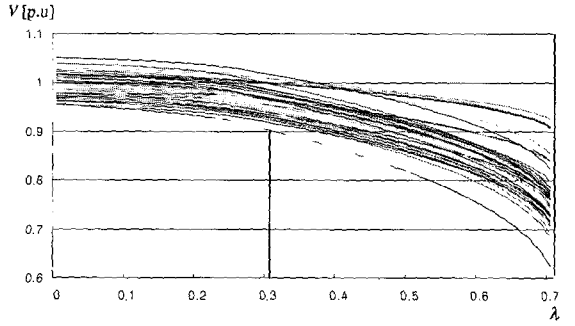

Fig. 18 Bus voltage versus λcurve

When STATCOM is installed on bus 31, which is a low voltage bus, λ is 0.705, which is a 0.069 increase compared to the value before installation is as shown in Fig. 18. If the bus voltage is above 0.9, λ increases 0.032 to a value of 0.307.

When fault occurs in the transmission line between bus 8 and bus 9, STATCOM is installed on bus 44 and 54 to increase the voltage stability margin.

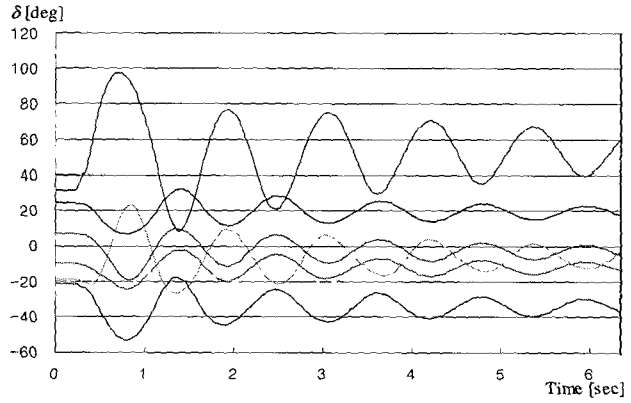

Fig. 19 Generator angle (Line 8-9 fault)

The maximum of λ is 0.483, and λ is 0.428 when the bus voltage is less than 0.9. The transient stability of the system is stable as presented in Fig. 19. This means that transfer power can be increased.

5. Conclusion

This paper has demonstrated a method of available transfer capability using CIM and Newton-Raphson on power systems with FACTS. This method applies the Newton method on the internal loop for FACTS so it does not require any modification of the existing program. However, it has a disadvantage of increasing the number of iterations.

In addition, the ATC calculation method taking in account dynamic characteristics of power systems has been proposed. It has been concluded that the ATC is increased by FACTS. More research is necessary for the identification of optimal installation location and optimal parameters.

References

[1] North American Electric Reliability Council(NERC), "Available Transfer Capability Definitions and Determination," June 1996

[2] G.C. Ejebe, J. Tong, J.G. Waight, J.G.Frame, X. Wang, and W.F. Tinney, "Available transfer capability calculations," IEEE Trans. on PS vol.13, no.4, pp1521-1527 , 1998

[3] J.B. Choo, B.H. Chang, H.S.Lee, H.S.Shin, K.K.Koh, "Development of FACTS operation technology to the KEPCO power Network," Transmission and Distribution conference and exhibition 2002 IEEE/PES vol.3, pp2008-2012 ; Oct. 2002

[4] B.A. Renz, A. Keri, A.S.Mehraban, C. Schauder. E. Stacey. L.Kovalsky, L. Gyugyi, A. Edris, "AEP Unifierd Power Flow Controller Performance," IEEE Trans. on PD, vol.14, no.4, pp1374-1381, Oct. 1999

[5] Z. X. Han, "Phase Shifter and Power Flow Control," IEEE Trans. on PAS, vol. 101, no. 10, pp3790-3795, Oct. 1982

[6] M. Noroozian, G. Anderson, "Power Flow Control by use of Controllable Series Components," IEEE/PES Summer Meeting, Seattle, WA,. pp12-16 , July, 1992

[7] N. Srinivasan, K. S. Prakasa Rao, C. S. Injulkar, S. S. Venkata, "On-Line Computation of Phase Shifter Distribution Factors and Line Load Allevation," IEEE Trans. on PAS, vol. 104, no. 7, pp 1656-1662, July, 1985

[8] Fuerte-Esquival, C. R. Acha, "Newton-Raphson

Algorithm for the Reliable Solution of Large Power Networks with Embedded FACTS Devices," Proc. IEE Pt. C, vol.143, no. 5, pp447-454 , 1996

[9] S. Arabi, P. Kundur, "Versatile FACTS Device Model for Power Flow and Stability Simulation," IEEE Winter Meeting, 1996

[10] Kalyan K. Sea, Eric J. Stacey, "UPFC-Unified Power Flow Controller: Theory, Modeling, and Application," IEEE Trans. on PD, vol.13, no.4, pp1453-1460, Oct. 1998

[11] L. Gyugyi, C.D. Schauder, S.L. Williams, T.R. Rietman, D.R. Torgerson, D.R. Edris, "The Unified Power Flow Controller: a New Approach to Power Transmission Control," IEEE Trans. on PD, vol.10, no2, pp1085-1093, April 1995

[12] K.S. Smith, L. Ran, J. Penman, "Dynamic Modeling of Unified Power Flow Controller," IEE Proc. GTD vol.144, no.1, pp7-12, Jan. 1997

[13] Z. Huang, Y. Ni, C.M. Shen, F. Wu, S. Chen, B. Zhang, "Application of Unified Power Flow Controller in Interconnected Power Systems - Modeling, Interface, Control Strategy, and Case Study," IEEE Trans. on PS, vol.15, no.2, pp817-824, May 2000

[14] H. Chiang, A.J. Flueck, K.S. Shah, N. Balu, "CPFLOW: A practical tool for tracing power system steady-state stationary behavior due to load and generation variations," IEEE Trans. on PS vol.10, no.2, pp623-634, 1995

[15] Yan OU, Chanan Singh, "Assessment of Available Transfer Capability and Margins," IEEE Trans. on PS, vol.17, no.2, pp463-468, May, 2002

[16] Allen J. Wood, Bruce F. Wollenberg, "Power Generation, Operation and Control", John Wiley & Sons, Inc., pp.430-432, 1996

[17] S. Arabi, P. Kunder, R.Adapa, "Innovative techniques in modeling UPFC for power system analysis", IEEE Trans. On PS, vol.15, no.1, pp336-341, Feb. 2000

[18] Karl Schoder, Area Hasanovic, Ali Feliachi, "Power System Damping Using Fuzzy Controlled Unified Power Flow Controller", IEEE PES Winter meeting, pp617-622, 2001

Jae-Hyeon Gim (M94)

He received his B.S. degree in Electrical Engineering from Hongik University, Seoul, Korea, in 1977 and his M.S. and Ph.D. degrees from the University of Texas, Arlington, TX, in 1989 and 1994, respectively. In 1994, he joined the Department of Electrical Control Engineering, Sunchon National University, Chonnam, Korea, where he has been involved in research on dynamic stability analysis, control of power systems and ATC.

Yang-Il Kim

He received his B.S. degree in the Department of Physics and his M.S. degree in the Department of Electrical Control Engineering from Sunchon National University, Chonnam, Korea, in 2000 and 2002, respectively. He is now pursuing a Ph.D. degree from Sunchon National University.

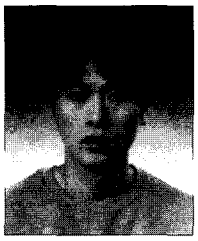

Sung-Won Jeung

He received his B.S. degree in the Department of Electrical Control Engineering from Sunchon National University, Chonnam, Korea, in 2001. He is now pursuing a M.S. degree from Sunchon National University.